Journal of Controlled Release 316 (2019) 250–262

Contents lists available at ScienceDirect

Journal of Controlled Release

journal homepage: www.elsevier.com/locate/jconrel

Targeted PEG-poly(glutamic acid) complexes for inhalation protein delivery to the lung

A. Nieto-Orellana[a,1], H. Li[a,1], R. Rosiere[b], N. Wauthoz[b], H. Williams[c], C.J. Monteiro[a], C. Bosquillon[a], N. Childerhouse[d], G. Keegan[d], D. Coghlan[d], G. Mantovani[a,*], S. Stolnik[a,*]

[a] Molecular Therapeutics and Formulation Division, School of Pharmacy, University of Nottingham, Nottingham, UK
[b] Laboratory of Pharmaceutics and Biopharmaceutics (ULBGAL), Université Libre de Bruxelles, Bruxelles, BE, Belgium
[c] Centre for Biomolecular Sciences, University of Nottingham, Nottingham, UK
[d] Vectura Group plc, Chippenhafm, UK

ARTICLE INFO

Keywords:
Polymer-protein complexes
Inhalation delivery
Spray-dried inhalation powder
Protein delivery
Targeted complexes

ABSTRACT

Pulmonary delivery is increasingly seen as an attractive, non-invasive route for the delivery of forthcoming protein therapeutics. In this context, here we describe protein complexes with a new 'complexing excipient' - vitamin B_{12}-targeted poly(ethylene glycol)-*block*-poly(glutamic acid) copolymers. These form complexes in sub-200 nm size with a model protein, suitable for cellular targeting and intracellular delivery. Initially we confirmed expression of vitamin B_{12}-internalization receptor (CD320) by Calu-3 cells of the *in vitro* lung epithelial model used, and demonstrated enhanced B_{12} receptor-mediated cellular internalization of B_{12}-targeted complexes, relative to non-targeted counterparts or protein alone. To develop an inhalation formulation, the protein complexes were spray dried adopting a standard protocol into powders with aerodynamic diameter within the suitable range for lower airway deposition. The cellular internalization of targeted complexes from dry powders applied directly to Calu-3 model was found to be 2–3 fold higher compared to non-targeted complexes. The copolymer complexes show no complement activation, and *in vivo* lung tolerance studies demonstrated that repeated administration of formulated dry powders over a 3 week period in healthy BALB/c mice induced no significant toxicity or indications of lung inflammation, as assessed by cell population count and quantification of IL-1β, IL-6, and TNF-α pro-inflammatory markers. Importantly, the *in vivo* data appear to suggest that B_{12}-targeted polymer complexes administered as dry powder enhance lung retention of their protein payload, relative to protein alone and non-targeted counterparts. Taken together, our data illustrate the potential developability of novel B_{12}-targeted poly(ethylene glycol)-poly(glutamic acid) copolymers as excipients suitable to be formulated into a dry powder product for the inhalation delivery of proteins, with no significant lung toxicity, and with enhanced protein retention at their *in vivo* target tissue.

1. Introduction

Pulmonary delivery is increasingly investigated as an alternative route for the delivery of bio-therapeutics, including proteins [1]. Several proteins and peptides - e.g. cyclosporine A to treat asthma, and interleukin-2 to treat pulmonary metastases of renal cell carcinoma [2,3] -have been investigated for delivery to the lung. In 2014, an inhaled insulin preparation Afrezza was approved by the US Food and Drug Administration [4], and is a currently available option in diabetes treatment. However, the lung presents specific barriers for macromolecular/protein therapeutics. Susceptibility to enzymatic degradation, poor absorption across epithelial barrier, as well as lung induced immunogenicity are significant challenges to be addressed if this approach is to be adopted as a viable alternative for protein delivery [5,6]. Covalent attachment of PEG (generally referred to as PEGylation) has evolved as the technique of choice in the bid to increase protein resistance to enzymatic degradation and reduced immunogenicity [7,8]. PEGylation has been shown to enhance protein absorption following nasal administration [9,10], and several studies showed promising delivery of PEGylated therapeutics to both the upper and lower respiratory tract for either systemic or local therapeutic effects [11,12].

To date, chemical conjugation to a therapeutic protein has been used in a vast majority of PEGylation studies [13,14]. However, it does not answer all the challenges of protein delivery, with a primary

* Corresponding authors.
E-mail addresses: giuseppe.mantovani@nottingham.ac.uk (G. Mantovani), snjezana.stolnik@nottingham.ac.uk (S. Stolnik).
[1] These authors contributed equally to this paper.

https://doi.org/10.1016/j.jconrel.2019.10.012
Received 4 June 2019; Received in revised form 2 September 2019; Accepted 6 October 2019
Available online 31 October 2019
0168-3659/

disadvantage being a potential decrease in the protein's therapeutic effect due to irreversible modification/steric shielding of its active site [15,16]. Non-covalent PEGylation, i.e. formation of protein–polymer non-covalent complexes has been explored as a potentially suitable alternative. In a seminal work from Kataoka's group, stable complexes in nanometer size range were assembled from PEG-polyanion or -polycation copolymers and charged macromolecules, including proteins [17]. Non-covalent PEGylated complexes were also produced from insulin and oligolysine or oligoarginine-type peptide polymers functionalized with PEG [18]. An alternative to non-covalent PEGylation based on electrostatic interactions between PEG-polyelectrolyte copolymer and selected protein, PEG bearing a terminal cholanic moiety ($mPEG_{5kDa}$-cholane) was utilized to generate polymer conjugates through non-covalent hydrophobic interactions with a range of protein and peptides, including recombinant human granulocyte colony stimulating factor (rh-G-CSF) [19], palmytoilated vasoactive intestinal peptide (VIP) [20], and recombinant human growth hormone (rh-GH) [21]. These non-covalent protein-polymer complexes can be assembled by simply mixing protein and polymer components under optimized conditions, avoiding the often complex conjugation chemistries required for covalent PEGylation. The intrinsically reversible nature of these interactions potentially allow complex disassembly under specific conditions - e.g. those found in the proximity of the intended biological target - which addresses the potential disadvantages covalent conjugation discussed above.

In this work, we present a further development in the non-covalent PEGylation approach, by engineering ligand-targeted non-covalent complexes which exploit cell-specific transport pathways for the intracellular delivery of therapeutic protein. To the best of our knowledge, this is the first example of ligand-targeted polymer-protein ionic complexes used for intracellular delivery of complexed protein.

Accordingly, here we engineered cyanocobalamin (vitamin B_{12}) ligand-targeted complexes based on B_{12}-PEG-poly(glutamic acid), using lysozyme as a model protein cargo. A family of B_{12}-PEG-poly(glutamic acid) copolymers with linear and miktoarm polymer topology was synthesized. These are used as a new 'complexing excipient' to assemble nano-sized complexes with the model protein, which can then be spray-dried into inhalable dry powders for inhalation delivery to the lung epithelium. In *in vitro* studies, Calu-3 cells were chosen as lung epithelial model and were grown as polarized layers in air-liquid interface culture (AIC) conditions to promote mucus secretion, normally considered to mimic lung physiological conditions [22]. Data show enhanced cellular internalization of targeted complexes, relative to non-targeted counterparts or 'free' protein. Toxicity studies demonstrated no complement activation, and *in vivo* lung tolerability assessment shows no significant signs of lung inflammation on repeated administration of formulated dry powders to healthy mice. *In vivo* lung deposition data illustrate ability of the complexes formulated as dry powders to deposit and retain model protein cargo in the lung tissue following pulmonary administration.

2. Methods

2.1. α-dibenzocyclooctyne-vitamin B_{12} (DBCO-B_{12})

Cyanocobalamin (vitamin B_{12}, 50 mg, 0.037 mmol, 1 eq.) was dissolved in anhydrous DMSO (5 mL) under inert atmosphere. 1,1′-carbonyldiimidazole (CDI) (9.7 mg, 0.060 mmol, 1.6 eq.) was then added, and the reaction was stirred at 30 °C for 1.5 h followed by addition of a solution of dibenzocyclooctyne-amine (30 mg, 0.11 mmol, 3 eq.) in DMSO (5 mL). The resulting solution was stirred at room temperature protected from light for 24 h. The mixture was then precipitated in diethyl ether, centrifuged, and the solid residue was dissolved in methanol and purified by preparative-TLC (^{i}PrOH : *n*-BuOH : H_2O : NH_4OH 30:45:21:4). The product was extracted from the relevant TLC band using methanol, then the resulting suspension was filtered, and after solvent removal under reduced pressure DBCO-B_{12} was isolated as a pink-red solid. Yield: 11 mg, 22 %. Mass spectrometry and RP HPLC (Supporting Information, Figure S1) confirmed the purity of the isolated DBCO-B_{12}: expected *m/z* [M-Na^{++}] theor. 851.85, found 851.33.

2.2. B_{12}-PEG_{3k}-*mik*-$(GA_{17})_3$ and B_{12}-PEG_{3k}-*lin*-(GA_{24})

Azide-PEG_{3k}-*mik*-$(GA_{17})_3$ (40 mg, 0.0022 mmol, 1 eq.) or azide-PEG_{3k}-*lin*-(GA_{24}) (100 mg, 0.013 mmol, 1 eq.) (Supporting Information, Figure S1 and S2) were dissolved in deionized water (3 mL). DBCO-B_{12} (7 mg, 0.004 mmol, 2 eq., or 44 mg, 0.026 mmol, 2 eq.) to form B_{12}-PEG_{3k}-*mik*-poly$(GA_{17})_3$ and B_{12}-PEG_{3k}-*lin*-(GA_{24}) copolymers, respectively was dissolved in DMSO (3 mL) and then added to the round bottom flask containing the relevant copolymer. The mixture was stirred at room temperature protected from the light overnight. The solution was then dialyzed (MWCO 3.5 kDa) against deionized water, and after freeze-drying B_{12}-PEG_{3k}-*mik*-$(GA_{17})_3$ and B_{12}-PEG_{3k}-*lin*-(GA_{24}) were isolated as pink solids.

2.3. B_{12}-PEG_{3k}-*mik*-$(GA_{17})_3$

Yield 39 mg, 91 %. ^{1}H NMR (400 MHz, D_2O, δ, ppm): 4.44-4.28 (bs, HNC*H*CO), 3.75-3.60 (s, OCH_2 of PEG), 2.52-1.90 (m, CH_2CH_2COOH). $M_{n,NMR}$ = 21.0 kDa, $M_{n,SEC}$ = 4.8 kDa, $Đ_{SEC}$ = 1.59. **B_{12}-PEG_{3k}-*lin*-(GA_{24})** yield: 121 mg, 96 %. ^{1}H NMR (400 MHz, D_2O, δ, ppm): 7.83-7.66 (s, C$H_{aromatic}$), 7.50-7.33 (s, C$H_{aromatic}$), 4.47-4.05 (bs, HNC*H*CO), 3.76-3.58 (s, OCH_2 of PEG), 2.50-1.86 (m, CH_2CH_2COOH). $M_{n,NMR}$ = 9.8 kDa, $M_{n,SEC}$ = 4.4 kDa, Đ = 1.23.

2.4. Untargeted $mPEG_{2k}$-polyGA copolymers

Linear $mPEG_{2k}$-*lin*-GA_{30} and miktoarm $mPEG_{2k}$-*mik*-$(GA_{10})_3$ copolymers were synthesized in our previous work [23].

2.5. Preparation of polymer-protein complexes

($mPEG_{2k}$-*lin*-GA_{30})-lysozyme complexes were prepared at relative molar charge ratios $r = 2.5$ where r is the charge ratio between the number of glutamic acid residues in the copolymer (negatively charged at physiological pH), and the 17 lysine and arginine residues (positively charged at physiological pH) of lysozyme. Polymers and protein were separately dissolved in phosphate buffer (PB, 10 mM, pH 7.4) and appropriate aliquots were mixed to achieve $r = 2.5$. For example, to make 1 mL of complexes at 70 μg mL^{-1} protein concentration for nanoparticle tracking analysis, 21 μg of $mPEG_{2k}$-*lin*-GA_{30} and 70 μg of lysozyme were mixed in 1 mL of 10 mM PB. Specific protein and polymer concentrations are reported in the description of individual experiments below.

To prepare targeted polymer-protein complexes, $mPEG_{2k}$-*lin*-GA_{30} and B_{12}-PEG-polyGA copolymers were mixed at relative molar ratios of 85:15 (mol:mol), respectively. Polymers mixture and lysozyme were then mixed at relative molar charge ratio of 2.5.

To monitor protein cellular uptake, lysozyme used in all subsequent studies was fluorescently labelled using sulfo-Cyanine 5 (Cy5) succinimidyl (NHS) ester (Lumiprobe), according to manufacturer protocol. After dialysis, protein concentration and degree of labelling were determined using dye:protein (F/P) molar ratios' equations as described in the Supporting Information.

2.6. Nanoparticle tracking analysis (NTA)

The hydrodynamic diameter of B_{12}-targeted and non-targeted polymer-protein complexes was measured by NTA (Nanosight LM14). All measurements were performed at 25 °C. NTA 2.0 Build 127 software was used for data acquisition and analysis. The samples were measured for 80 s. Mean size ± SD values correspond to the arithmetic values

calculated for all the particles analyzed by the software. Polymer-protein complexes were prepared at charge ratios of 2.5 in 10 mM phosphate buffer, pH 7.4. Protein concentration was kept constant (70 μg mL^{-1}) for all measurements. Free protein and polymers were used as controls.

2.7. Formulation of complexes as dry powders by spray-drying

The complexes were formulated into dry powders following procedure optimized previously [24]. The composition of dry powders was: 0–10 % (w/w) protein-polymer complexes, 10 % (w/w) leucine, 6.6 % (w/w) phosphate buffer salts, and trehalose as bulking agent (up to 100 % (w/w)).

2.8. Cell culture

Human airway epithelial cells (Calu-3) were routinely cultured in DMEM/F-12 medium. Medium was supplemented with Foetal Bovine Serum (FBS, 10 % *v/v*), non-essential aminoacids (1 % *v/v*), L-glutamine (1 % *v/v*), penicillin (100 units mL^{-1}) and streptomycin (0.1 mg mL^{-1}). DPBS and trypsin/EDTA were used to wash and detach adherent cells in the process of cell splitting. Cells were always incubated at 37 °C and 5 % CO_2.

2.9. Culture of cells on Transwell® inserts

Calu-3 cells were seeded at 1×10^6 cells cm^{-2} on Transwell® inserts (12 mm diameter, 0.4 μm pore size; Corning Life Sciences, USA) and cultured for 14 days, with medium replacement every two days. Cells were cultured using air-interface culture (AIC) conditions [22] known to promote mucus secretion, starting from day 2 post-seeding on Transwell® inserts. Cell confluence and cell layer integrity before treatments with test samples was confirmed by transepithelial electrical resistance (TEER) measurements (EVOM voltohmmeter, World Precision Elements, USA). Cells included in the experiments always had values higher than 550 Ω cm^{-2}.

2.10. cDNA synthesis and quantitative PCR analysis

Total RNA was extracted using RNeasy Mini Kit (Qiagen, Hilden, Germany) according to manufacturer's instructions. RNA concentration and purity were assessed using NanoDrop spectrophotometer (Thermo Scientific, Wilmington, DE). Five-hundred nanograms of total RNA were reverse transcribed to complementary DNA (cDNA) by QuantiTect Reverse Transcription Kit (Qiagen). Genomic DNA elimination was carried out twice, during RNA extraction and before the cDNA synthesis. qPCR reactions were performed in 96-well white-walled plates using 2x Brilliant II SYBR® Green QPCR Master Mix (Agilent) with the following primer sets: cubilin forward primer: 5′-CGTGGAACACACAA ACTTTAGG-3′ and reverse primer: 5′-CCAGTGAGGGGATCTGATTG-3′; TCN2 receptor (CD320) forward primer: 5′-CACCCACCAAGTTCCAGT GCCG-3′ and reverse primer: 5′-GTTCCACAGCCGAGCTCGTCG-3′; TCN2 forward primer: 5′-GCTGGTTGTGGCACAGTA-3′ and reverse primer: 5′-AGGTCCACAGGCCATCAAT-3′. Glyceraldehyde-3-phosphate dehydrogenase (GAPDH) was used as a standardization control (forward primer: 5′-AGGTGAAGGTCGGAGTCAAC-3′ and reverse primer: 5′-GATGACAAGCTTCCCGTTCT-3′). ΔΔCq method was used to calculate relative gene expression.

2.11. Cellular uptake of pyr-B12 fluorescent probe

Calu-3 and Caco-2 cells were cultured on Transwell® inserts over 14 and 21 days, under air-liquid or liquid-liquid interface respectively. Culture medium was removed from filter-cultured cells and replaced with Hank's Balanced Salt Solution (HBSS) in both Transwell® compartments for TEER measurements. Following the measurement of TEER, pyr-B_{12} probe (synthesized as described in the Supporting Information) was dissolved in DMEM medium without phenol red at concentration of 200 μg mL^{-1}, and 500 μL of this solution was added to the apical chamber of the Transwell® insert. Cells were then incubated at 37 °C for 3 h and analyzed by flow cytometry (Beckman Coulter Astrios EQ) in at least triplicate experiments, with more than 10,000 cells measured in each sample.

The effect of a competitive ligand on receptor-mediated cellular internalization of fluorescent pyr-B_{12} probe was studied in the presence of an excess of free vitamin B_{12}; 500 μL of a 1.0 mg mL^{-1} solution of cyanocobalamin (B_{12}) in DMEM medium was added to the apical chamber of Transwell® inserts. Cells were subsequently incubated at 37 °C for 30 min, then the medium was replaced with a stock solution of fluorescent pyr-B_{12} probe (500 μL, final probe concentration 200 μg mL^{-1}) plus free vitamin B_{12} at the same concentration as the pre-incubation solution. Cells were incubated at 37 °C for 3 h, fixed with formaldehyde and analyzed by flow cytometry (Beckman Coulter Astrios EQ). Experiments were made in at least triplicates, with more than 10,000 cells measured in each sample.

2.12. Cellular internalization of polymer-protein complexes applied as suspension

Calu-3 cells were cultured on Transwell® inserts over 14 days as described above. Culture medium was removed and replaced with Hank's Balanced Salt Solution (HBSS) prior to the experiment. Polymer-protein complexes were applied as a suspension in HBSS at concentration of 3 μg mL^{-1} protein. Following TEER measurement (to assess cell layer integrity), the complexes suspension (0.5 mL) was added to the apical chamber of the Transwell® insert. Cells were then incubated at 37 °C for 3 h and fixed with 2% formaldehyde followed by analysis by flow cytometry in at least quadruplicate experiments, with more than 10,000 cells measured in each sample.

The effect of a competitive ligand on receptor-mediated uptake of B_{12} targeted complexes was studied in the presence of an excess of free cyanocobalamin (vitamin B_{12}). Firstly, 500 μL of a 1.0 mg mL^{-1} solution of cyanocobalamin (B_{12}) in HBSS was added to the apical chamber of quadruplicate Transwell® inserts. Cells were then incubated at 37 °C for 30 min following addition of targeted polymer-protein nanocomplex suspension (500 μL, final protein concentration 3 μg mL^{-1}). Cells were incubated again at 37 °C for 3 h, washed and fixed before analyzed by flow cytometry. Experiments were made in at least quadruplicate, with more than 10,000 cells measured in each sample.

2.13. Cellular internalization of protein-polymer complexes applied as dry powder formulations

Calu-3 cells were cultured on Transwell® inserts as previously described. Dry powders were sprayed twice (2 mg *per* dose) using a Dry Powder Insufflator™ model DP4-M® (Penn-Century®) into the Transwell® inserts as follows. Four Transwell® inserts were placed into a desiccator at equal distance from the center [25] (also illustrated in Supporting information, Figure S13). 2 mg of dry powder formulations were then sprayed twice from a Penn-Century® device. Next, 500 μL of Hank's Balanced Salts Solution (HBSS) were added to the basolateral chamber of the Transwell® inserts and cells were incubated at 37 °C and 5% CO_2 for 3 h. Cells were then detached with trypsin/EDTA, washed twice with DPBS, fixed with 2% formaldehyde and lysozyme uptake was analyzed by flow cytometry in quadruplicate experiments, with more than 10,000 cells measured in each sample.

2.14. In vitro assessment of complement activation

[B_{12}-PEG-*lin*-(GA_{30})]-lysozyme complexes or free lysozyme were incubated with normal human serum (NHS) and the residual hemolytic capacity was measured to study the complement activation. NHS was

received from healthy volunteers (Phlebotomy Department, Nottingham University Hospitals, NHS Trust) and, once sensitized, suspended at a final concentration of 1×10^8 cells mL^{-1} in veronal-buffer saline (VBS^{2+}, containing 0.5 mM Mg^{2+} and 0.15 mM Ca^{2+}). VBS^{2+} and NHS were mixed with lysozyme-polymer complexes or free lysozyme at a final protein concentration of 1.12 mg mL^{-1} so that the final dilution of NHS in the reaction mixture was 1/4 (v/v) in a final volume of 400 μL. The suspension was incubated at 37 °C for 60 min under gentle stirring. The mixture was then diluted 1/25 (v/v) in VBS^{2+} and aliquots at different dilutions were added to a specific volume of sensitized sheep erythrocytes. The suspensions were incubated for 45 min at 37 °C under gentle stirring and the reaction was then stopped by adding ice-cold NaCl (0.15 M). The mixture was centrifuged at 2000 rpm for 5 min to precipitate un-lysed erythrocytes. The supernatant was collected and the optical density was measured at λ = 415 nm (Cary Eclipse Spectrophotometer).

Mixture of sensitized sheep erythrocytes in VBS^{2+} without NHS was used here as positive control and employed to correct the baseline absorbance values. Mixture of sensitized sheep erythrocytes with addition of distilled water which would result in total hemolysis was utilized as negative control. In this study, the data were expressed as the percentage of complement activation relative to 100 % complement activation observed with the positive control samples.

2.15. In vivo evaluation of the complexes formulated as dry powders

2.15.1. Animals and husbandry conditions

Female BALB/c mice (Charles River, Arbresle, France) were kept under conventional housing conditions (22 ± 2 °C, 55 ± 10 % humidity, and 12 -h day/night cycle). All studies and manipulations were approved by the CEBEA ethical committee of the Faculty of Medicine, ULB (Commission d'Ethique du Bien-Etre Animal, Université libre de Bruxelles, Belgium) (Ethical protocol N°585 N). The laboratory federal agreement number is LA 1230568.

2.15.2. Characterisation of dry powder formulations emitted by the dry powder insufflator

Aerosol particles generated from Dry Powder Insufflator™ model DP4-M® (Penn-Century®, Philadelphia, USA) were confirmed to be suitable for endotracheal administration into the mice by using a Spraytec® laser diffractometer. The emitted aerosol, created using Dry Powder Insufflator™ model DP4-M®, was presented dispersed in air directly and perpendicular to the laser beam for size measurement. For all formulations tested (Table 1) a loading powder mass of 2 mg was evaluated (n = 10). High emitted mass values (> 80%), particle size D50 ≤ 5 μm and RSD values ≤ 25% for emitted masses were considered suitable for the administration of dry powder formulations to the mice (Supporting information, Table S1).

2.15.3. Local pulmonary tolerance of the complexes

Solution of LPS and dry powder formulations were administered by the non-invasive endotracheal route using an aerosolizing system (Microsprayer™ model IA-1C®) or a dry powder insufflator designed for mice (Dry Powder Insufflator™ model DP4-M®, Penn-Century), respectively, as described elsewhere [26,27].

Composition of formulations tested is shown in Table 1. Five groups were compared: (i) non-treated mice negative control (i.e. group baseline, n = 6), (ii) mice treated with unlabeled dry powder (denoted as UDP) (control dry powders, with no protein nor copolymers, excipients only) (n = 5), (iii) mice treated with unlabeled dry powder-protein (UDP-P) (dry powders containing lysozyme, but not polymers) (n = 5), (iv) mice treated with unlabeled dry powder containing protein-targeted complexes (UDP-TC) (dry powders containing 85:15 [$mPEG_{2k}$-*lin*-GA_{30}/B_{12}-PEG_{3k}-*lin*-(GA_{24})]-lysozyme complexes) (n = 5), and (v) mice treated with a lipopolysaccharide (LPS) solution (single administration of 1 μg dose) as positive control (n = 6). Mice were treated with 2 mg dose of dry powders three time a week for three consecutive weeks.

Bronchoalveolar lavage fluids (BALFs) were analyzed in terms of cell composition (total and differential cell count) and pro-inflammatory markers concentration (cytokines IL-1β, IL-6, and TNF-α), as previously described [27]. Mice were euthanized by a lethal intraperitoneal injection of 12 mg sodium phenobarbital (Nembutal®, Ceva Santé Animale, Brussels, Belgium) 8 h (for the LPS group) or 24 h (for the dry powder inhaler groups) after the last inhaled administration. BALFs were collected using a 20-gauge cannula (Surflo® catheter, Terumo, Leuven, Belgium) with 3 flushes of 0.7 mL cold PBS and conserved on ice until total cell count analysis (Z2™ Coulter Counter®, Beckman Coulter, Suarlée, Belgium). BALF were centrifuged at 160 x g at 4 °C, supernatants were collected and conserved at −80 °C for cytokine quantification. Differential cell counts were performed on cytospin preparations after staining with May Grünwald and Giemsa (Sigma-Aldrich). A total of 200 cells were counted per slide and were referred to as alveolar macrophages, lymphocytes or polymorphonuclear neutrophils according to their morphology. Cytokine concentrations were determined by ELISA for mouse IL-1 β, IL-6, and TNF-α (DuoSet® ELISA, RnD Systems) according to the manufacturer's protocols. The limits of quantification for the techniques used were 15.6 pg mL^{-1} for IL-1β and IL-6, and 31.3 pg mL^{-1} for TNF-α.

2.15.4. In vivo pulmonary deposition and retention

The deposition of the dry powder formulations was evaluated after pulmonary delivery. Lysozyme-Cy5-containing DPI formulations (LDP-P, LDP-TC and LDP-NT, composition in Table 1) were administered to mice (2 mice *per* group) by the endotracheal route, as described above. After 0, 3 and 14 h, mice were sacrificed using sodium pentobarbital, the lungs were collected and blocked using Optimum Cutting

Table 1
Composition of dry powder formulations used in the *in vivo* studies.

	Formulation code	Lysozyme/Complexes (w/w)	Leucine (% w/w)	Excipients Buffer salts (% w/w)	Trehalose (% w/w)
unlabeled dry powder (UDP)	UDP	0 % complexes	10	6	Up to 100
	UDP-P	5 % lysozyme	10	6	Up to 100
	UDP-TC	10 % targeted complexes[a]	10	6	Up to 100
Cy5 labelled dry powder (LDP)	LDP-P	5 % lysozyme	10	6	Up to 100
	LDP-TC	10 % targeted complexes[a]	10	6	Up to 100
	LDP-NT	10 % non-targeted complexes	10	6	Up to 100

UDP-P denotes dry power containing unlabeled protein, UDP-TC denotes dry power containing unlabeled protein complexes with B_{12}-targeted polymer, LDP-TC denotes dry powder containing labelled protein complexes with B_{12}-targeted polymers, LDP-NT denotes dry powder containing labelled protein with non-targeted polymer.
Unlabeled dry powder formulations were used for local pulmonary tolerance studies, and Cy5-labelled protein dry powder formulations were used for pulmonary deposition and retention studies.
[a] corresponding to ~ 5% w/w of lysozyme.

Temperature (OCT) solution (Tissue-Tek® OCT compound, Sakura). Five non-serial cryo-sections of 7 μm *per* lung were prepared and mounted on SuperFrost™ slides (Thermo Fischer Scientific) using a DAPI solution (DAPI Counterstain, Abott Laboratories, Des Plaines, IL, USA) and finally covered with a coverslip. The slides were observed under a Leica SP8 confocal microscope (Leica Microsystems, Diegem, Belgium) with filters (Zeiss, Germany) at 546 nm (bandwidth 12 nm) and 610 nm (bandwidth 65 nm) used for excitation and emission, respectively, for Cy5 labelled protein. Due to sub-optimal spectral overlap, prolonged exposure (1000 ms) was needed to acquire images. A DAPI filter (Zeiss) was used for DAPI. The images were processed (i.e. fluorescence intensity, mean grey values) using ImageJ Software (National Institutes of Health, USA). Quantitative data are presented as the ratio of average of the grey mean values of Cy5 to DAPI areas (n = 5 tissue slices), as described in Dawson et al [28].

3. Results and discussion

Delivery of therapeutic macromolecules into, or across cells forming epithelial barrier is a recognized therapeutic challenge. Potential solutions include approaches that exploit normal biological pathways of cellular internalization and transcytosis of nutrients, vitamins, as well as macromolecules [29,30]. In our previous study, we demonstrated that vitamin B_{12} can i) be used as a ligand to enhance internalization of model sub-200 nm polystyrene particles by epithelial cells, ii) influence their intracellular trafficking pathways, and iii) enhance transport of decorated nanoparticles across Calu-3 cell layer [31,32]. Here, we apply the B_{12} directed cellular internalization and transport to achieve targeted delivery of polymer-protein complexes *in vitro* and *in vivo*. Accordingly, we synthesized a family of targeted B_{12}-PEG_{3k}-polyGA copolymers and utilized these to generate polymer-protein complexes *via* ionic, non-covalent interactions between polymer and model protein charged functionalities.

3.1. Synthesis of targeted B_{12}-PEG-polyGA copolymers

The B_{12}-targeted copolymers, B_{12}-PEG-polyGA (Fig. 1), were produced through a modification of an approach we developed previously for synthesis of analogous non-targeted counterparts (Supporting information, Figures S2 and S3) [23]. The synthesis of both linear and miktoarm B_{12}-targeted polymers started from *O*-(2-aminoethyl)polyethylene glycol (3.0 kDa), and involved *N*-carboxyanhydride (NCA) polymerization of γ-benzyl-L-glutamate *N*-carboxyanhydride (NCA) to generate, after hydrolysis of the benzyl ester protecting groups, a poly (glutamic acid) polyanion block. B_{12}-targeted copolymers were prepared from a 3 kDa PEG block, which is longer than the 2 kDa PEG used for the non-targeted analogues, to potentially increase the exposure of B_{12} ligands at the surface of the corresponding protein-polymer complexes.

In the final step, the required B_{12} ligand was introduced in linear azide-PEG_{3k}-*lin*-(GA_{24}) **(1)** and miktoarm azide-PEG_{3k}-*mik*-$(GA_{17})_3$ **(2)** intermediates by copper-free strain-promoted Huisgen 1,3-dipolar cycloaddition (Supporting information, Figures S2 and S3) [33,34]. To this aim, α-dibenzocyclooctyne-vitamin B_{12} (DBCO-B_{12}) was synthesized by activating the CH_2OH group at C_5 of cyanocobalamin pentose moiety with carbonyldiimidazole(CDI) for 30 min in DMSO, followed by the addition of commercially available α-dibenzocyclooctyne-amine, to form a stable carbamate linker. Reaction with the azide-containing intermediates **(1)** and **(2)** in water-DMSO followed by dialysis afforded the final linear B_{12}-PEG_{3k}-*lin*-(GA_{24}) and miktoarm B_{12}-PEG_{3k}-*mik*-$(GA_{17})_3$ protein-complexing copolymers (Fig. 2).

The successful click conjugation of DBCO-B_{12} to azide-PEG_{3k}-*b*-polyGA was confirmed by 2D Heteronuclear Single-Quantum Correlation (HSQC) and 1D ^{1}H NMR (Fig. 3). Due to the complexity of the NMR spectra of B_{12}-PEG_{3k}-*lin*-(GA_{24}) and B_{12}-PEG_{3k}-*mik*-poly $(GA_{17})_3$ copolymers, model low molecular weight azides and

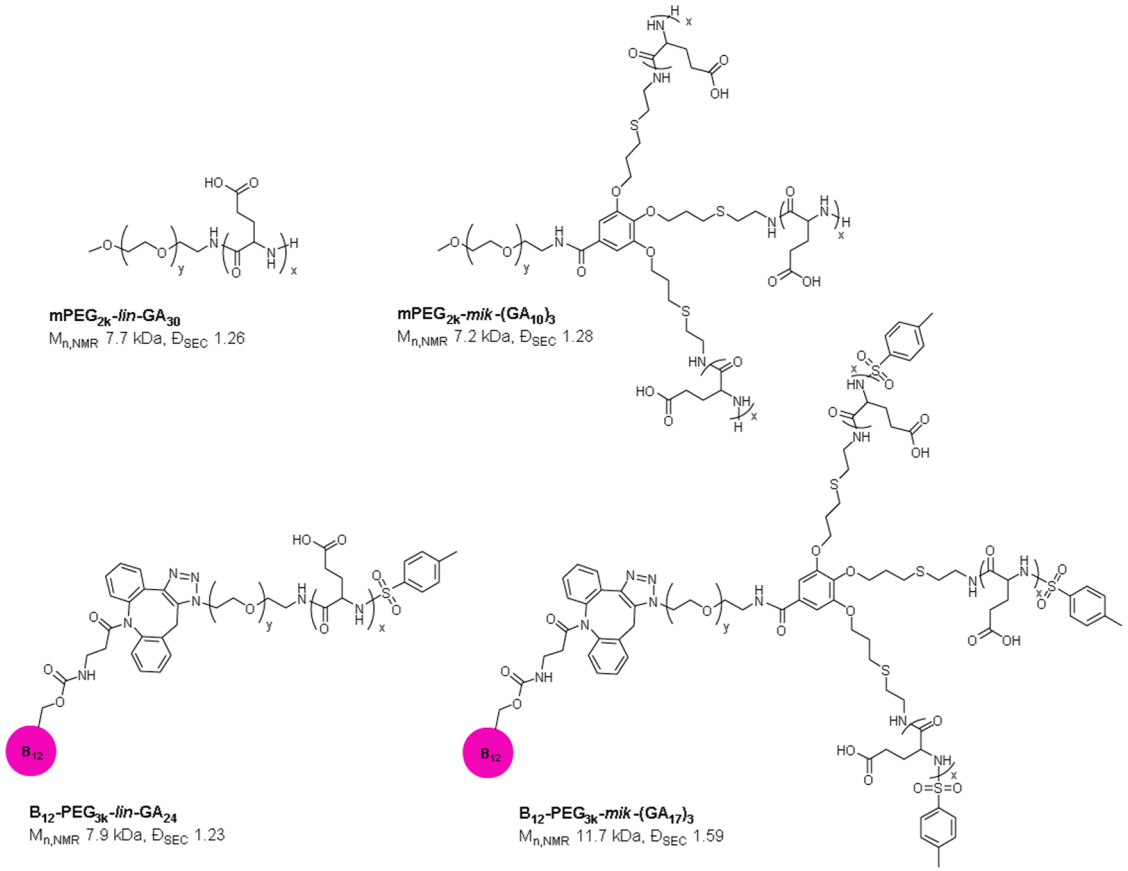

Fig. 1. Chemical structure of non-targeted (top), and B_{12}-targeted (bottom) PEG-poly(glutamic acid) copolymers with linear and miktoarm topology.

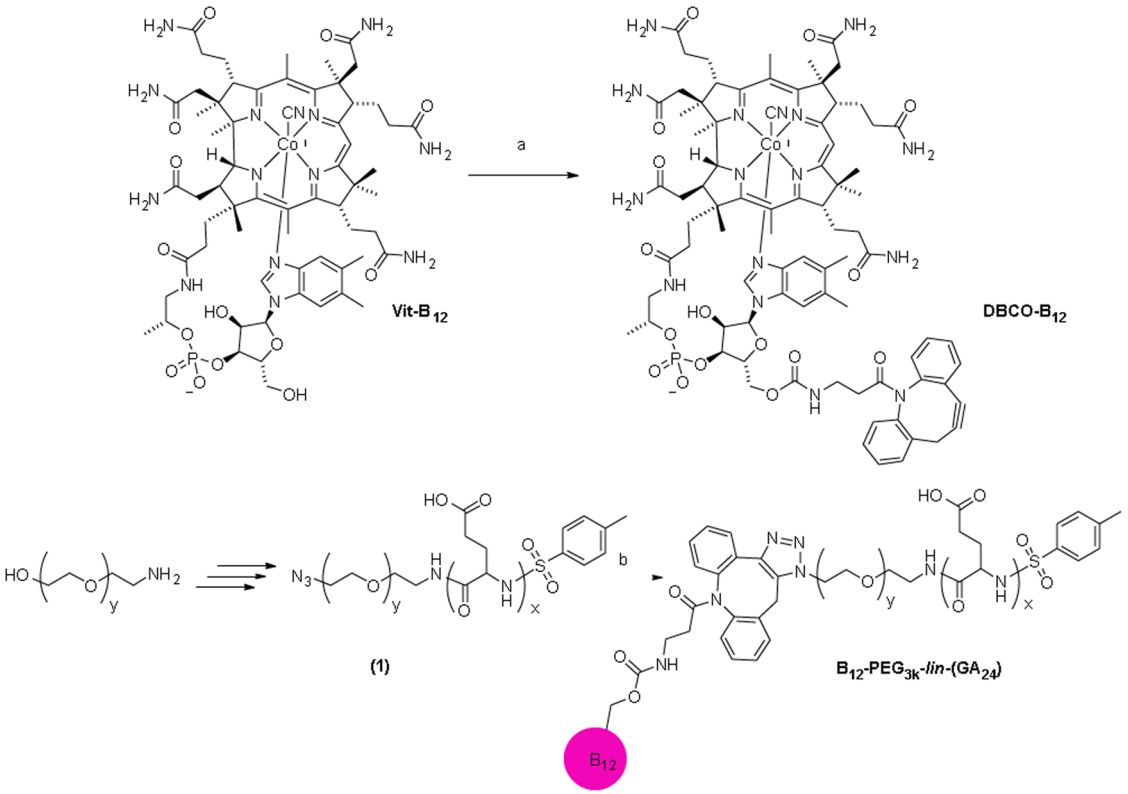

Fig. 2. Synthesis of vitamin B_{12}-targeted B_{12}-PEG_{3k}-*lin*-(GA_{24}) copolymers. Reactions and conditions: a) i. 1,1′-carbonyldiimidazole, ii. dibenzocyclooctyne-amine (DBCO-amine) b) DBCO-B_{12}, DMSO/H_2O, overnight. B_{12}-PEG_{3k}-*mik*-$(GA_{17})_3$ was prepared in an analogous manner, from miktoarm azide-PEG_{3k}-*mik*-$(GA_{17})_3$ intermediate (2) (Supporting information, Figure S2).

cyclooctynes were synthesized and analyzed to identify diagnostic peaks which would allow us to monitor this reaction (Supporting information, Figure S6). The α-CH2 protons of the cyclooctyne ring were found to be particularly suitable for this, due to their relatively large ^{1}H NMR downfield shift (~ 0.7-0.8 ppm) following click cycloaddition (Fig. 3).

More specifically, one of the two α-CH_2 protons of α-dibenzocyclooctyne-B_{12} (DBCO-B_{12}) at 5.0 and 56 ppm, for ^{1}H and ^{13}C, respectively, was found to shift to 5.9 and 52 ppm, following click cycloaddition with linear N_3-PEG_{3k}-*lin*-(GA_{24}) azide precursor **(1)**, which confirmed successful conjugation. For the miktoarm B_{12}-PEG_{3k}-*mik*-poly(OBn-$GA_{17})_3$ copolymer, although the quality of the HSQC NMR data was not suitable for confirming the presence of the desired product due to a poor signal intensity, 1D ^{1}H NMR indicate the appearance of the diagnostic signal at 5.9 pm for the clicked B_{12} adduct, thus confirming the success of the click reaction. Size exclusion chromatography

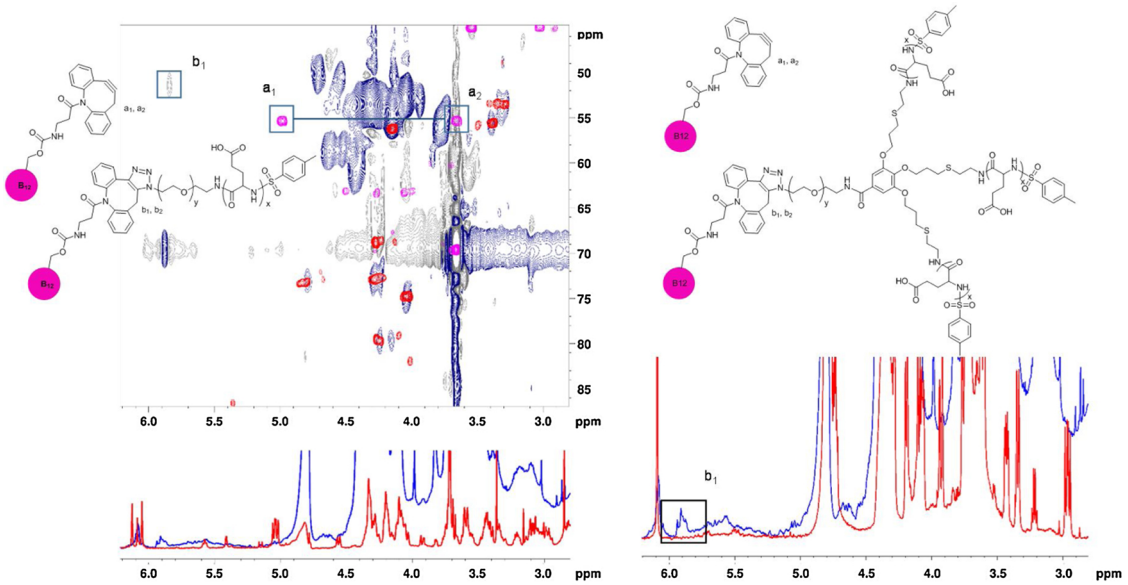

Fig. 3. ^{1}H NMR and HSQC spectra of the α-CH_2 proton signal of the α-dibenzocyclooctyne-amine before (a1, a2) and after (b1, b2) the copper-free click conjugation of DBCO-B_{12} to azide-PEG_{3k}-*lin*-(GA_{24}) (1) (left) and azide-PEG_{3k}-mik-$(GA_{17})_3$ (2) (right).

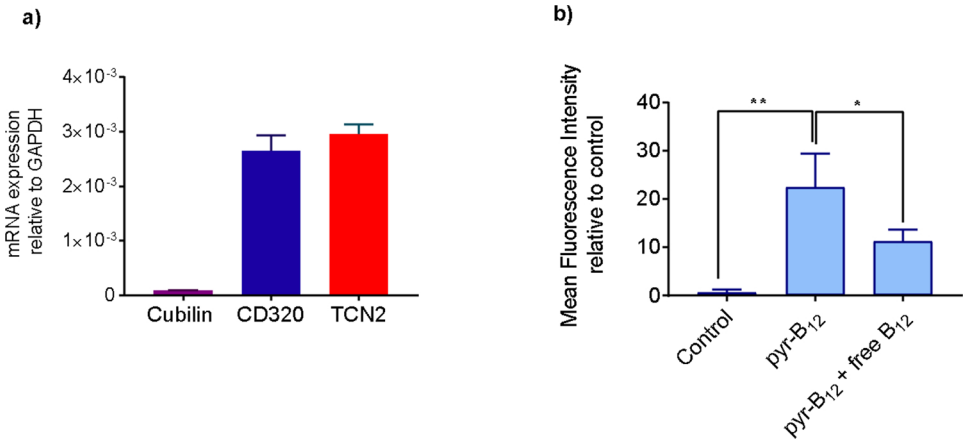

Fig. 4. a) mRNA expression of cubilin, CD320 and TCN2 relative to GAPDH (as housekeeping gene) by Calu-3 cells. b) Cellular internalization of pyr-B_{12} fluorescent probe by Calu-3 cells in the presence or absence of free vitamin B_{12} competitive ligand. Control: untreated cells. One-way ANOVA was used for statistical analysis. *P ≤ 0.05, **P ≤ 0.01, ***P ≤ 0.001, **** P ≤ 0.0001. Flow cytometry conducted at λ_{ex} 401 nm and λ_{em} 421 nm.

of the purified final polymers confirmed complete removal of the excess of unreacted α-dibenzocyclooctyne-B_{12} (Supporting information, Figure S4), whilst efficiency of functionalization was estimated by UV–vis spectrometry (λ = 540 nm) at 93 and 97% for linear B_{12}-PEG_{3k}-*lin*-(GA_{24}) and miktoarm B_{12}-PEG_{3k}-*mik*-$(GA_{17})_3$, respectively.

3.2. Targeted PEG-poly(GA)-lysozyme complexes

PEG-poly(GA) copolymer-protein complexes with lysozyme as a model protein cargo were assembled using a mixture of B_{12}-targeted and non-targeted PEG-poly(GA) copolymers. In this study a 15:85 molar ratio, respectively was selected. We appreciate that the density of surface exposed targeting ligand, and indeed its clustering, has a profound effect on nanoparticles internalization, as illustrated in previous research from our and other groups. Using another nano-sized targeted system with folate ligand we previously achieved a reasonable level of cellular internalization for a range of ligand 'surface functionalization' [33], and based on that a 15:85 ratio was considered as a good starting point. A polymer-protein relative molar charge ratio of 2.5 - defined as the molar ratio between glutamic acid polymer repeating units, assumed to be all negatively charged at pH 7.4, and cationic amino acids of lysozyme – was used, as we have previously shown efficient complexation of PEG-poly(GA) copolymers to lysozyme under these conditions [23]. The data (Supporting information, Figures S10 and S11) indicate a formation of polymer-protein complexes in the 120–180 nm size range - suitable size for endocytosis - for targeted and non-targeted systems, as assessed by nanoparticle tracking analysis (NTA). Gel electrophoresis analysis of complexes suspended in cell culture medium shows that majority of lysozyme remains complexed during 3 h of cellular internalization study, when suspended in cell growth medium, and is released on change in pH to 4.5 in simulated lysosomal environment (Supporting information, Figure S12).

3.3. Expression of mRNA and function of B_{12} receptors

The presence of components involved in vitamin B_{12}-specific transport pathways has been widely confirmed in intestinal epithelium models, such as *in vitro* cultures of Caco-2 cells [34,35], and B_{12} receptors have been successfully targeted for intestinal delivery of proteins [36,37], and *in vitro* transport of nanoparticles across intestinal epithelium. In the latter, B_{12} transport can occur through two different receptors: cubilin and transcobalamin receptor (CD320, or TCN2R) [38]. Evidence of vitamin B_{12} transport mechanisms in the lung epithelium, and its *in vitro* cell models, is scarce. We have previously demonstrated, using a combination of molecular biology and immunostaining techniques, that Calu-3 bronchial cell line expresses the B_{12}-IF receptor (cubilin), the transcobalamin receptor ('TCN2 receptor', CD320), and the transcobalamin II protein ('TCN2') [31]. The present work confirms (Fig. 4a) at mRNA level, expression of cubilin (human CUBN gene), transcobalamin receptor (CD320 gene) and transcobalamin II protein (human TCN2 gene). mRNA expression of the cubilin receptor was found to be very low, relative to control gene expression. It should be noted that the mechanism of vitamin B_{12} uptake *via* cubilin receptor requires the initial complexation of B_{12} with Intrinsic Factor (IF, or Gastric Intrinsic factor, GIF), a glycoprotein that is produced by parietal cells in the stomach [39]. Thus, it may not be surprising that cubilin-dependent transport pathway would be downregulated in Calu-3 cells, which originate from the lung tissue. Conversely, transcobalamin receptor (CD320)-mediated transport requires initial binding of vitamin B_{12} to TCN2 carrier protein, followed by uptake of the resulting complex by CD320 (transcobalamin) receptor-mediated endocytosis [40,41]. The TCN2 protein in this complex is eventually degraded in the lysosomes, releasing cobalamin (vitamin B_{12}) which is further processed intracellularly [40]. In this work, expression of mRNA for transcobalamin II protein in Calu-3 cell culture was confirmed by qPCR (Fig. 4a) while in a previous study we have shown TCN2 protein expression in Calu-3 cells in a qualitative manner, by immunostaining [31]. Taken together, our results indicate that Calu-3 cell model used in this study possess all the functional components required for cellular internalization of cobalamin (vitamin B_{12}) molecules *via* transcobalamin (CD320) receptor-mediated transport.

To confirm functional, endocytic activity of vitamin B_{12} receptors in Calu-3 epithelial model employed in this study, we designed a low molecular weight B_{12}-fluorescent probe, pyr-B_{12}. This O-alkyl pyranine-based fluorescent compound was selected due to its structural similarity to Lucifer Yellow, which is known to have low cell membrane permeability, while possessing functionalities appropriate for conjugating to vitamin B_{12}. Accordingly, *O*-alkyl pyranine blue-fluorescent dye with narrow Stokes shift (λ_{ex} = 401 nm, λ_{em} = 421 nm), was linked to the 5′ hydroxyl group of the ribose ring of cyanocobalamin, in a similar way to the approach followed for the synthesis of DBCO-B_{12}, in four steps, starting from 8-hydroxypyrene-1,3,6-trisulfonic acid trisodium salt (pyranine), and cyanocobalamin (B_{12}) (Supporting Information, Figure S8). For comparative purposes, in another experiment cellular internalization of pyr-B_{12} by the established cell model expressing both cubilin and TCN2 B_{12} receptors, intestinal Caco-2 cell line [42,43], was also assessed (Supporting Information, Figure S9). Data in Fig. 4b show a significant reduction of pyr-B_{12} cellular internalization in the presence of an excess of 'free' vitamin B_{12} competitive ligand. This indicates a prominent, but not exclusive, role of B_{12}-specific transport in the cellular internalization of pyr-B_{12} probe, likely occurring through TCN2 receptor mediated transport.

3.4. Complement activation

An undesired effect associated with pulmonary delivery is the

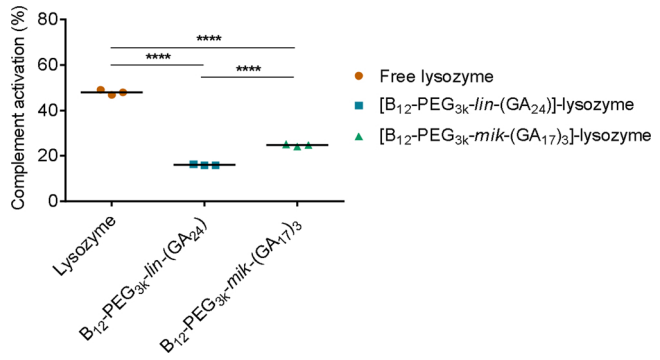

Fig. 5. Complement activation by free lysozyme, linear [85:15 $mPEG_{2k}$-*lin*-GA_{30}/B_{12}-PEG_{3k}-*lin*-(GA_{24})]-lysozyme and miktoarm [85:15 $mPEG_{2k}$-*mik*-$(GA_{10})_3$/B_{12}-PEG_{3k}-*mik*-$(GA_{17})_3$]-lysozyme complexes. The data expressed as the percentage of complement activation relative to 100% complement activation observed with the positive control samples (where no haemolysis have occurred). Lysozyme concentration was kept constant to 1.12 mg mL^{-1} for all samples. One-way ANOVA was used for statistical analysis. *** $p < 0.001$, **** $p < 0.0001$.

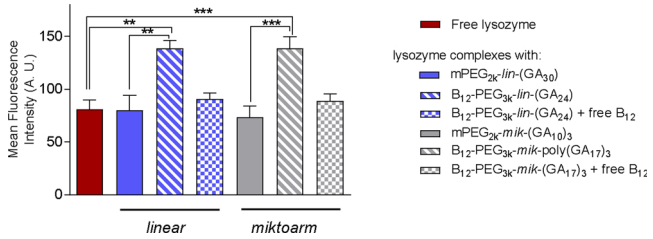

Fig. 6. Cellular internalization of B_{12}-targeted and non-targeted PEG-poly(GA)-Cy5-lysozyme complexes by Calu-3 cells grown as polarized epithelial cell layers. Suspensions of complexes were applied at protein concentration of 3 μg mL^{-1} and incubated with cells for 3 h prior to flow cytometry analysis. Cells were grown as polarized layers on Transwell supports under air-liquid interface conditions. '+ free B_{12}' denotes presence of excess of soluble B_{12} competitive ligand in the medium, 'free lysozyme' indicates that cells were treated with a solution of Cy5-lysozyme in the absence of PEG-poly(GA) complexing copolymers. One-way ANOVA was used for statistical analysis. ** $p < 0.01$, *** $p < 0.001$.

immunogenicity of drug delivery systems, protein cargoes, or both. Accordingly, immunogenic formulations/proteins can lead to reduced efficacy, inflammation, anaphylaxis and autoimmunity. These side-effects can result from a range of factors, including the intrinsic nature of specific protein therapeutics, and their tendency to aggregate, either during storage or *in vivo*, which leads to their increased immunogenicity [44–46]. The complement system has key roles in innate and adaptive immune responses. Although most complement proteins are generated in the liver as inactive precursor enzymes, the lung may also act as a local source of complement proteins [47]. In this study normal human serum was selected as a source of complement proteins, due to the ease of serum availability compared to the extraction of complement proteins present in the lungs. The ability of free lysozyme and B_{12}-targeted lysozyme complexes to activate the complement system was evaluated (Fig. 5). At the concentration investigated (1.12 mg mL^{-1}), 'free' lysozyme was found to activate the complement system to around 50% level, whilst for lysozyme complexes with targeted B_{12}-PEG_{3k}-poly(GA) polymers, these values decreased to 16 and 25% when linear or miktoarm copolymers were used, respectively (Fig. 5).

PEG is known to decrease protein immunogenicity, following covalent PEG-protein conjugation [48]. Therefore, the reduction in immunogenic response observed for the PEG-poly(GA)-lysozyme complexes could be ascribed to the similar effect of steric stabilization provided by PEG chains on the complexed lysozyme. Interestingly, linear polymer showed somewhat higher protection than miktoarm copolymers, potentially indicating some differences in their complexation with the protein. Taken together, these results suggest that protein complexation with PEG-poly(GA) copolymers can reduce the complement activation triggered by model protein, lysozyme, and that, within specific contexts, this approach could potentially serve as a strategy to reduce immunogenicity of protein therapeutics.

3.5. Cellular internalization of B_{12}-targeted protein-polymer complexes in vitro

Data in Fig. 6 demonstrate significantly increased cellular internalization of targeted B_{12}-PEG_{3k}-poly(GA)-protein complexes, compared to 'free' Cy5-lysozyme or non-targeted $mPEG_{2k}$-poly(GA)-lysozyme complexes. Interestingly, this effect was independent on the topology of the complexing polymers - linear B_{12}-PEG_{3k}-*lin*-(GA_{24}), *vs.* miktoarm B_{12}-PEG_{3k}-*mik*-$(GA_{17})_3$. Importantly, cellular internalization of targeted complexes decreased significantly in the presence of an excess of 'free' vitamin B_{12} competitive ligand, confirming a prominent, but not exclusive, role of a vitamin B_{12}-specific transport mechanism in the complexes trafficking by cells.

The observed level of cellular internalization of' free' cy5-lysozyme (Fig. 6) was somewhat unexpected. Data on similar experiments on cellular uptake of lysozyme are scarce, but recent *in vivo* studies reported on absorption of lysozyme in the intestinal tract [49], which appears to be occurring by non-saturable and saturable processes, the latter pointing to an involvement of endocytic pathway(s). Furthermore, it has recently been suggested that receptor-mediated endocytosis of lysozyme in renal proximal tubules may be mediated by megalin and cubilin [50]; the mRNA expression, although at a very low level, of the latter receptor was confirmed in the cell model used in this study. Furthermore it should be noted that complexation of lysozyme with non-targeted copolymers resulted in similar level of internalization as for 'free' lysozyme (Fig. 6), a result that would be unexpected if one considers that PEGylation is generally recognized to reduce cellular uptake of colloidal size particulates [51]. As noticed above, the B_{12}-mediated pathway does not appear to be an exclusive transport mechanism for tested systems in the cellular model used, and hence further studies to decipher internalization pathways would be needed, e.g. [52]. These are however beyond the scope of the current work that aims to design targeted excipients for inhalable dry powder formulations.

It should be noted that our study used polarized, differentiated epithelial cell layer grown at air-liquid interface, and although a number of previous reports studied intracellular delivery of self-assembled protein carrying systems, these are conducted on a variety of non-polarized cells, such as HeLa and dendritic cells [53,54], which makes direct comparisons difficult.

Aiming at developing inhalable formulations, we spray-dried PEG-poly(GA)-protein complexes using a 'standard' process and excipients. In these formulations, trehalose was selected as the matrix excipient due to its well characterized ability to stabilize biologics. When spray dried, trehalose creates an amorphous matrix that forms hydrogen bonds with biologic materials and protects structural integrity following the removal of water. Other excipients that are approved for inhalation formulations, such as mannitol and lactose, are known to crystallize when spray dried, limiting their ability to provide a protective amorphous matrix. The amorphous nature of trehalose renders the particles hygroscopic and highly cohesive. This limits the ability of passive inhalers to efficiently disperse the powder to a respirable size (< 5 μm aerodynamic diameter) for lung delivery. Leucine is a surface active amino acid that accumulates at the surface of the droplet during the spray drying process. This results in high concentrations of leucine

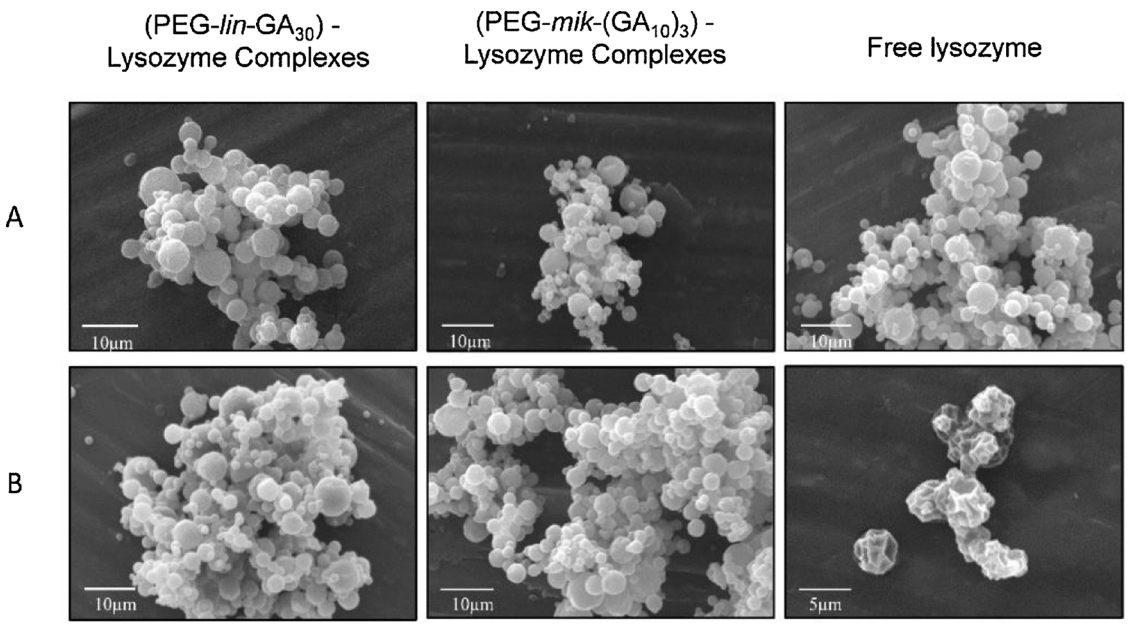

Fig. 7. Scanning electron microscopy images of PEG-poly(GA)-lysozyme complexes formulated as dry powders by spray drying. Upper row A) dry powder formulations prior spraying and lower row B) following spraying of formulated dry powders through a Penn-Century® insufflator device. All dry powders contain 6.6% (w/w) phosphate salts, 10% (w/w) leucine and up to 100% (w/w) trehalose. Image for free lysozyme after spraying through Penn-Century® insufflator is presented at enlarged scale to emphasize morphology change.

localized to the particle surface in comparison to the particle interior. This deposition changes the properties of the spray dried particle, decreasing cohesion and therefore reducing the energy required to efficiently disperse the powder to a respirable size during inhalation. The addition of leucine dramatically improves the fine particle fraction achievable from the device, directly translating into improved deposition properties of the powder [24]. The resulting formulations possessed aerodynamic properties suitable for inhalable product, with particle size (D_{50}) < 5 µm (Supporting information, Table S1). 10% loading level was selected to ensure stability of the nano-complexes during the spray drying process and to maintain efficient aerosol performance. In this instance, the powders exhibited comparable aerosol performance when formulated as the placebo formulation (trehalose and leucine) and as the nano-complex loaded powder (loaded at 10% level), indicating that inclusion of the nano-complexes did not change the particle properties. These formulations were shown to maintain lysozyme biological activity [24]. They were applied as dry powders to Calu-3 cell layers grown at air-liquid interface, and in *in vivo* studies, by Penn-Century® insufflator device. Particle morphology, size and size distribution prior and following spraying by the insufflator are shown in Fig. 7 (and Supporting Information, Tables S1, S2 and Figure S14). SEM images in Fig. 7 illustrate spherical particle shape of dry powders prior and following spraying with insufflator device for formulations prepared with PEG-poly(GA)-lysozyme complexes. Interestingly, some loss of spherical morphology for powders containing 'free' lysozyme is seen, indicating in turn that complexation of the protein with PEG-poly(GA) provided a level of structural stabilization of the formulations.

In line with the results obtained for cells treatment with suspensions of PEG-poly(GA)-protein complexes (Fig. 6), application of respective dry powders demonstrates a significantly higher cellular internalization of targeted [B_{12}-PEG_{3k}-poly(GA)]-Cy5-lysozyme complexes, relative to 'free' lysozyme, or non-targeted complexes (Fig. 8). The results hence indicate that i) B_{12}-targeted PEG-poly(GA)-lysozyme complexes can be formulated into dry powders by spray drying process, ii) the complexation somewhat protects the powder morphology on subsequent exposure to spraying, and iii) B_{12}-targeted complexes are released from dry powders formulations under aqueous conditions, to then be internalized by the epithelial cells.

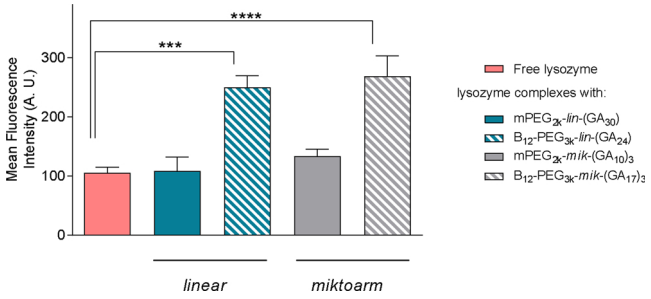

Fig. 8. Cellular internalization of B_{12}-targeted and non-targeted PEG-poly(GA):Cy5-lysozyme complexes formulated into dry powders in *in vitro* Calu-3 epithelial model. Samples were applied as dry powders using dry powder insufflator (PenCentury insufflator) directly onto apical side of the Calu-3 cells grown as polarized layers on Transwell supports under air-liquid interface conditions (Supporting information, Figure S13). 'Free lysozyme' denotes dry powder formulated from Cy5-lysozyme in the absence of complexing polymers. All dry powders contain phosphate buffer salts (6.6% w/w), leucine (10% w/w) and trehalose (up to 100% w/w). One-way ANOVA was used for statistical analysis. *** $p < 0.001$, **** $p < 0.0001$.

3.6. Local pulmonary tolerance of polymer-protein complexes-based dry powder formulations in healthy mice

The safety profile of PEG-poly(GA)-lysozyme complexes formulated as dry powder inhalable formulations was investigated in healthy mice. Previous reports have shown that administration of polymer-based pulmonary formulations can induce inflammatory responses [55,56], whilst the presence in dry powder formulations of poorly soluble material has been shown to induce local irritation and pro-inflammatory

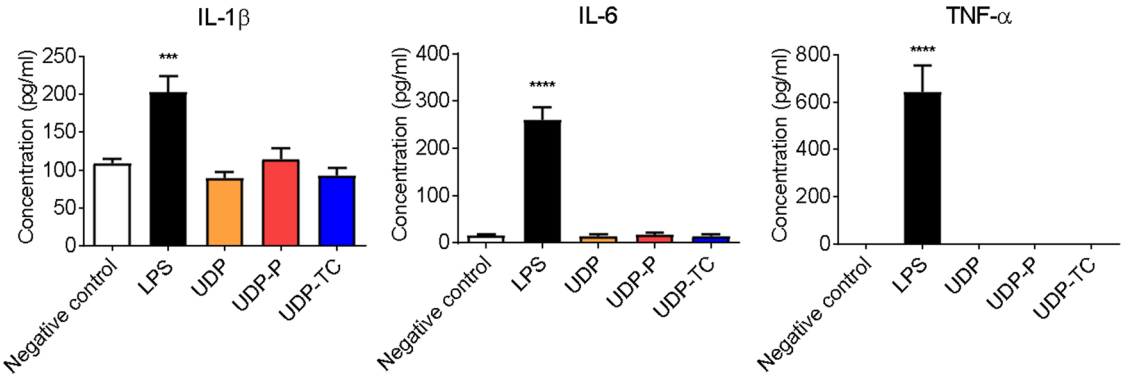

Fig. 9. Pro-inflammatory cytokine IL-1β, IL-6, and TNF-α gene expression in lung tissues following administration of 2 mg of dry powder formulations 3 times a week for 3 weeks. Mice groups were untreated (negative control) or treated with LPS (positive control), treated with a formulation containing only dry powder excipients (UDP), free lysozyme formulation containing lysozyme and dry powder excipients (UDP-P), and dry powder formulation containing targeted complexes (UDP-TC) - with 85:15 [$mPEG_{2k}$-*lin*-GA_{30}/B_{12}-PEG_{3k}-*lin*-(GA_{24})]-lysozyme composition. One-way ANOVA was used for statistical analysis. *** $p < 0.001$, **** $p < 0.0001$.

effect in the respiratory tract [57,58]. In addition, the delivery of proteins to the lungs has been shown to induce immunogenicity, local irritation and toxicity [59–61]. In this work, we evaluated the lung tolerance profile of PEG-poly(GA)-lysozyme dry powders in healthy BALB/c mice, by quantifying cell count and local concentration of IL-1β, IL-6 and TNF-α cytokine in bronchoalveolar lavage fluids after endotracheal administrations of 2 mg of dry powders 3 times *per* week, for 3 weeks period. The dose and the administration schedules were established taking into account limitations of the preclinical mice model. Aimed, and achieved, administration of 2 mg (Supporting information, Table S1), corresponds to a dose of ~100 mg/kg of powder mass and ~10 mg/kg protein – within a range potentially expected of a therapeutic protein to be delivered in humans. The administration schedule was devised taking into account limitations associated with general anaesthesia of mice during endotracheal instillation and their well-being. 48 h (i.e. three doses per week) was previously assessed as the minimum interval between two such administration procedures [62,63]. Systems tested included: dry powder formulation of [$mPEG_{2k}$-*lin*-GA_{30}/B_{12}-PEG_{3k}-*lin*-(GA_{24})]-lysozyme targeted complexes (UDP-TC), formulation containing only dry powder excipients (UDP), and system containing 'free' lysozyme formulated with dry powder excipients but with no polymers to complex the protein (UDP-P) (the compositions of these formulations are shown in Table 1).

Firstly, the potential inflammatory response of these formulations was investigated by quantification of the concentration of IL-1β, IL-6, and TNF-α pro-inflammatory cytokines [64,65], in the epithelial lining fluid of the lungs. Mice treated with lipopolysaccharide (LPS) - outer membrane component of Gram-negative bacteria known as a strong stimulator of innate or natural immunity [66] - were used as a positive control group. As expected, a significant increase in IL-1β, IL-6, and TNF-α level was observed on LPS treatment, compared to untreated mice (Fig. 9). The levels of measured cytokines did not increase significantly above the negative control level (untreated mice group) following administration of dry powder formulations. The data hence clearly illustrate that on a repeated, prolonged administration the tested PEG-poly(GA)-based formulations are well tolerated.

To further investigate the tolerability of the designed dry powder formulations upon pulmonary administration, the differential cell count of alveolar macrophages (AM), polymorphonuclear neutrophils (PMN), and lymphocytes (LM) was also performed (Fig. 10). Following single administration of 1 μg LPS, the number of AM dramatically decreased to around 50% relative to untreated mice, whereas the percentage of PMN significantly increased, clearly indicating a pro-inflammatory reaction. On the contrary, all the dry powder formulations had values for AM, PMN and LM at the level similar to untreated mice control. This was qualitatively confirmed by optical microscopy observations (Fig. 10). These experiments thus suggest that, under the conditions investigated, B_{12}-PEG-poly(GA)-lysozyme complexes-based dry powder formulations are well tolerated in the lungs following endotracheal administration, with no significant toxicity or lung inflammation observed.

3.7. *In vivo pulmonary deposition and retention of polymer-protein complexes-based dry powder formulations in healthy mice*

Pulmonary delivery of particle formulations can be challenging, due to different particle clearance mechanisms present at various levels of the airway path in the lungs, such as the mucociliary escalator, proteolytic degradation and macrophage capture [67]. However, a design of drug delivery system can potentially overcome these removal mechanisms [67] and, by prolonging the time of exposure of lung tissue to relevant protein therapeutics, enhance their therapeutic effects. In this part of our study, the ability of PEG_{3k}-(GA_{24})-lysozyme complexes to increase the retention of proteins in the lungs was assessed.

Accordingly, a 2 mg dose of dry powder formulation (Supporting information, Table S2, Figure S14) was administered to healthy mice by the endotracheal route, using a Penn-Century insufflator. Fig. 11 shows the lung distribution of Cy5-labelled lysozyme following administration of dry powder formulation containing free Cy5-labelled lysozyme (LDP-P), dry powder formulation containing non-targeted $mPEG_{2k}$-*lin*-(GA_{30})-labelled lysozyme complexes (LDP-NT), and dry powder formulation containing 85:15 [$mPEG_{2k}$-lin-GA_{30}/B_{12}-PEG_{3k}-*lin*-(GA_{24})]-lysozyme targeted complexes (LDP-TC). Five non-serial cryo-sections of 7 μm thickness *per* lung were prepared, imaged by fluorescence microscopy (Supporting Information, Figure S15), and representative examples are shown in Fig. 11. Images depict that immediately following administration (at t = 0 h) Cy5-lysozyme powders were indeed deposited in the lungs, which agrees with the previous studies reporting that dry powders with good dispersion properties can be deposited in the respiratory zone in the mouse lungs [68]. Fluorescent images obtained from different lung tissue sections however indicate that the deposition was not homogeneous throughout the lung (Supporting Information Figure S15), which increases complexity in making comparisons between the systems tested. This non-homogeneous deposition pattern have also been observed in other studies [63,69,70]. However, analysis of the images (Fig. 11, graph) indicates that in different samples imaged at 14 h after the administration of dry powders the fluorescence arising from Cy5-lysozyme is higher, relative to nuclear DAPI

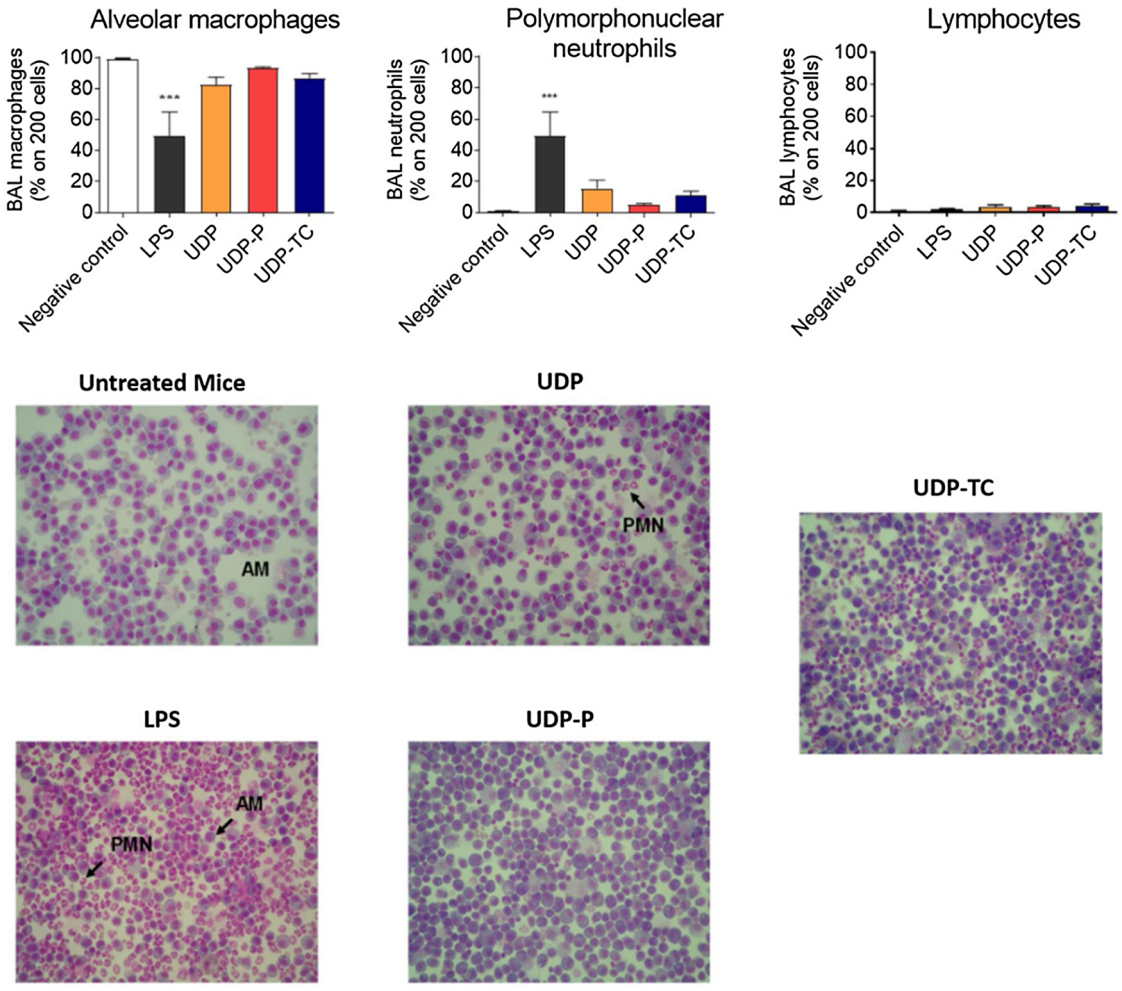

Fig. 10. Bronchoalveolar lavage fluid analysis following a single administration of dry powder formulations. Differential cell count and representative images of different cells found in the bronchoalveolar lavage fluid. Mice groups were: not treated, (negative control) or treated with single administration of 1 μg LPS (positive control), and 2 mg of dry powder formulation containing formulation excipients (UDP), free lysozyme dry powder formulation (UDP-P), or dry powder formulation containing targeted complexes (UDP-TC) [with composition of 85:15 $mPEG_{2k}$-lin-GA_{30}/B_{12}-PEG_{3k}-lin-(GA_{24})]-lysozymes] 3 times a week for 3 weeks. One-way ANOVA was used for statistical analysis. *** $p < 0.001$, **** $p < 0.0001$.

staining, for targeted complexes formulations (LDP-TC) in comparison to formulations containing 'free' (LDP-P) and non-targeted Cy5-lysozyme complexes (LDP-NT). This would indicate lengthier protein lung retention for the targeted formulation. All data considered, the lung deposition experiment provides an initial evidence of prolonged protein retention following administration of vitamin B_{12}-targeted complexes. Further studies are needed to confirm if this prolonged retention is indeed a consequence of the increased cellular internalization of targeted complexes seen in the *in vitro* cell culture experiment, and if this would lead to a potentially improved therapeutic effect of such delivered protein in the lung. Nevertheless, the *in vivo* deposition experiment suggests that targeted polymer-protein complexes can influence and potentially extend retention time of the protein cargo in the lungs.

4. Conclusions

In this study, we assessed the potential of vitamin B_{12} ligand-targeted poly(ethylene glycol)-*block*-poly(glutamic acid) copolymers to self-assemble with a protein cargo into polymer-protein complexes, with the aim to design an inhalation product with prolonged lung retention and intracellular delivery of protein to the lung epithelium. Our study shows that PEG-poly(GA)-protein complexes did not trigger significant complement activation, nor did they induce an increased production of pro-inflammatory cytokines in a chronic, repeated administration study in heathy mice. Furthermore, no changes in cell count of alveolar macrophages, polymorphonuclear neutrophils and lymphocytes, relative to untreated control, were observed that would indicate development of an inflammation process in the lung. Hence, toxicity data demonstrate that PEG-poly(GA) polymers based formulations are well tolerated in the lungs following chronic treatment, with no significant toxicity or lung inflammation indications.

The data demonstrate a B_{12}-receptor mediated internalization of B_{12} ligand-targeted PEG-poly(GA)-protein complexes *in vitro* in differentiated, polarized Calu-3 cells epithelial model. When fabricated into dry powders for inhalation using a standard spray drying procedure, and applied *in vivo*, the deposition data show prolonged lung retention of the protein cargo at 14 h after administration for targeted B_{12}-PEG-poly(GA)-protein complexes, relative to non-targeted or 'free' protein formulations. Taken together the results presented in this study show that vitamin B_{12}-PEG-poly(GA) copolymers have a potential as a new class of targeted 'excipients' for inhalation delivery of protein drugs to the lungs.

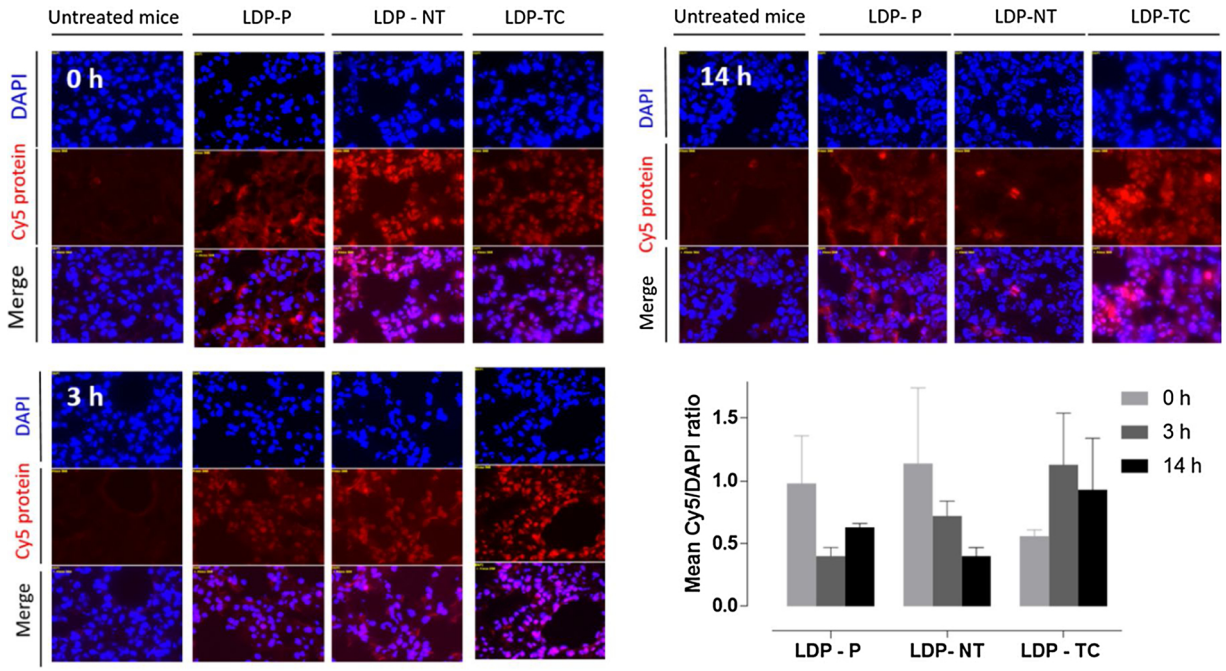

Fig. 11. Distribution of fluorescent labelled protein in the lung tissue of healthy mice following endotracheal application using the pulmonary delivery device of 2 mg dry powder formulations at different times after administration (in hours). Examples of a 7-μm longitudinal, non-consecutive lung cryo-sections imaged using a fluorescent microscope at 200 x magnification are shown (also in Supporting Information Figure S15). The images show the distribution of red labelled lysozyme-Cy5 ('Cy5 protein'), blue nuclear stain ('DAPI') and merged images ('Merged'); LDP-TC denotes dry powder formulation of [85:15 $mPEG_{2k}$-lin-GA_{30}/B_{12}-PEG_{3k}-lin-(GA_{24})]-lysozyme complexes, LDP-NT drug powder formulation of [$mPEG_{2k}$-lin-GA_{30}]-lysozyme non-targeted complexes, and LDP-P denotes free protein dry powder (without complexing polymers) formulation. Graph shows calculated ratio of Cy5 to DAPI emission intensity, obtained by analysis of images from 5 non-serial, random cryo-sections *per* lung (adopted from Dawson et al [28]). Low ratio for LDP-TC at 0 h illustrates the effect of non-homogeneous lung deposition on material present in the cryo-sections prepared for in the analysis. (For interpretation of the references to colour in this figure legend, the reader is referred to the web version of this article.).

Acknowledgements

Vectura Group plc and the School of Pharmacy at the University of Nottingham are acknowledged for funding Alejandro Nieto-Orellana and Huitong Li's PhD studentships. The authors would like to thank Dr. Ruggero Foralosso for providing insight and expertise that assisted the research.

Data created during this research are openly available from the corresponding authors (snjezana.stolnik@nottingham.ac.uk and giuseppe.mantovani@nottingham.ac.uk) and at the University of Nottingham Research Data Management Repository (https://rdmc.nottingham.ac.uk/), and data supporting this study are provided as supplementary information accompanying this paper.

Appendix A. Supplementary data

Supplementary material related to this article can be found, in the online version, at doi:https://doi.org/10.1016/j.jconrel.2019.10.012.

References

[1] J.S. Patil, S. Sarasija, Pulmonary drug delivery strategies: a concise, systematic review, Lung India 29 (2012) 44–49.
[2] S. Rohatagi, F. Calic, N. Harding, M.L. Ozoux, J.P. Bouriot, S. Kirkesseli, L. DeLeij, B.K. Jensen, Pharmacokinetics, pharmacodynamics, and safety of inhaled cyclosporin A (ADI628) after single and repeated administration in healthy male and female subjects and asthmatic patients, J. Clin. Pharmacol. 40 (2000) 1211–1226.
[3] O. Merimsky, E. Gez, R. Weitzen, H. Nehushtan, R. Rubinov, H. Hayat, T. Peretz, M. Ben-Shahar, H. Biran, R. Katsenelson, V. Mermershtein, D. Loven, N. Karminsky, A. Neumann, D. Matcejevsky, M. Inbar, Targeting pulmonary metastases of renal cell carcinoma by inhalation of interleukin-2, Ann. Oncol. 15 (2004) 610–612.
[4] D.C. Klonoff, Afrezza inhaled insulin: the fastest-acting FDA-approved insulin on the market has favorable properties, J. Diabetes Sci. Technol. 8 (2014) 1071–1073.
[5] M.P. Baker, H.M. Reynolds, B. Lumicisi, C.J. Bryson, Immunogenicity of protein therapeutics: the key causes, consequences and challenges, Self Nonself 1 (2010) 314–322.
[6] A. Hussain, J.J. Arnold, M.A. Khan, F. Ahsan, Absorption enhancers in pulmonary protein delivery, J. Control. Release 94 (2004) 15–24.
[7] A. Abuchowski, J.R. McCoy, N.C. Palczuk, T. van Es, F.F. Davis, Effect of covalent attachment of polyethylene glycol on immunogenicity and circulating life of bovine liver catalase, J. Biol. Chem. 252 (1977) 3582–3586.
[8] P.L. Turecek, M.J. Bossard, F. Schoetens, I.A. Ivens, PEGylation of biopharmaceuticals: a review of chemistry and nonclinical safety information of approved drugs, J. Pharm. Sci. 105 (2016) 460–475.
[9] Y.S. Youn, J.E. Jeon, S.Y. Chae, S. Lee, K.C. Lee, PEGylation improves the hypoglycaemic efficacy of intranasally administered glucagon-like peptide-1 in type 2 diabetic db/db mice, Diabetes Obes. Metab. 10 (2008) 343–346.
[10] T.H. Kim, C.W. Park, H.Y. Kim, M.H. Chi, S.K. Lee, Y.M. Song, H.H. Jiang, S.M. Lim, Y.S. Youn, K.C. Lee, Low molecular weight (1 kDa) polyethylene glycol conjugation markedly enhances the hypoglycemic effects of intranasally administered exendin-4 in type 2 diabetic db/db mice, Biol. Pharm. Bull. 35 (2012) 1076–1083.
[11] M.A. Croyle, A. Patel, K.N. Tran, M. Gray, Y. Zhang, J.E. Strong, H. Feldmann, G.P. Kobinger, Nasal delivery of an adenovirus-based vaccine bypasses pre-existing immunity to the vaccine carrier and improves the immune response in mice, PLoS One 3 (2008) e3548.
[12] M.N. Sahib, Y. Darwis, K.K. Peh, S.A. Abdulameer, Y.T. Tan, Rehydrated sterically stabilized phospholipid nanomicelles of budesonide for nebulization: physicochemical characterization and in vitro, in vivo evaluations, Int. J. Nanomedicine 6 (2011) 2351–2366.
[13] K. Kataoka, T. Matsumoto, M. Yokoyama, T. Okano, Y. Sakurai, S. Fukushima, K. Okamoto, G.S. Kwon, Doxorubicin-loaded poly(ethylene glycol)-poly(beta-benzyl-L-aspartate) copolymer micelles: their pharmaceutical characteristics and biological significance, J. Control. Release 64 (2000) 143–153.
[14] J.K. Dozier, M.D. Distefano, Site-specific PEGylation of therapeutic proteins, Int. J. Mol. Sci. 16 (2015) 25831–25864.
[15] A. Kato, S. Tanimoto, Y. Muraki, K. Kobayashi, I. Kumagai, Structural and functional properties of hen egg-white lysozyme deamidated by protein engineering, Biosci. Biotechnol. Biochem. 56 (1992) 1424–1428.
[16] J.A. Rodriguez-Martinez, R.J. Sola, B. Castillo, H.R. Cintron-Colon, I. Rivera-Rivera, G. Barletta, K. Griebenow, Stabilization of alpha-chymotrypsin upon PEGylation correlates with reduced structural dynamics, Biotechnol. Bioeng. 101 (2008) 1142–1149.
[17] A. Harada, K. Kataoka, Novel polyion complex micelles entrapping enzyme

molecules in the core: preparation of narrowly-distributed micelles from lysozyme and poly(ethylene glycol) – poly(aspartic acid) block copolymer in aqueous medium, Macromolecules 31 (1998) 288–294.
[18] D. Tsiourvas, Z. Sideratou, N. Sterioti, A. Papadopoulos, G. Nounesis, C.M. Paleos, Insulin complexes with PEGylated basic oligopeptides, J. Colloid Interface Sci. 384 (2012) 61–72.
[19] S. Salmaso, S. Bersani, F. Mastrotto, G. Tonon, R. Schrepfer, S. Genovese, P. Caliceti, Self-assembling nanocomposites for protein delivery: supramolecular interactions between PEG-cholane and rh-G-CSF, J. Control. Release 162 (2012) 176–184.
[20] E. Ambrosio, M. Barattin, S. Bersani, S. Shubber, S. Uddin, C.F. van der Walle, P. Caliceti, S. Salmaso, A novel combined strategy for the physical PEGylation of polypeptides, J. Control. Release 226 (2016) 35–46.
[21] S. Salmaso, S. Bersani, A. Scomparin, A. Balasso, C. Brazzale, M. Barattin, P. Caliceti, A novel soluble supramolecular system for sustained rh-GH delivery, J. Control. Release 194 (2014) 168–177.
[22] C.I. Grainger, L.L. Greenwell, D.J. Lockley, G.P. Martin, B. Forbes, Culture of Calu-3 cells at the air interface provides a representative model of the airway epithelial barrier, Pharm. Res. 23 (2006) 1482–1490.
[23] A. Nieto-Orellana, M. Di Antonio, C. Conte, F.H. Falcone, C. Bosquillon, N. Childerhouse, G. Mantovani, S. Stolnik, Effect of polymer topology on non-covalent polymer-protein complexation: miktoarm versus linear mPEG-poly(glutamic acid) copolymers, Polym. Chem. 8 (2017) 2210–2220.
[24] A. Nieto-Orellana, D. Coghlan, M. Rothery, F.H. Falcone, C. Bosquillon, N. Childerhouse, G. Mantovani, S. Stolnik, Dry-powder formulations of non-covalent protein complexes with linear or miktoarm copolymers for pulmonary delivery, Int. J. Pharm. 540 (2018) 78–88.
[25] E. Cingolani, S. Alqahtani, R.C. Sadler, D. Prime, S. Stolnik, C. Bosquillon, In vitro investigation on the impact of airway mucus on drug dissolution and absorption at the air-epithelium interface in the lungs, Eur. J. Pharm. Biopharm. 141 (2019) 210–220.
[26] M. Bivas-Benita, R. Zwier, H.E. Junginger, G. Borchard, Non-invasive pulmonary aerosol delivery in mice by the endotracheal route, Eur. J. Pharm. Biopharm. 61 (2005) 214–218.
[27] R. Rosiere, M. Van Woensel, V. Mathieu, I. Langer, T. Mathivet, M. Vermeersch, K. Amighi, N. Wauthoz, Development and evaluation of well-tolerated and tumor-penetrating polymeric micelle-based dry powders for inhaled anti-cancer chemotherapy, Int. J. Pharm. 501 (2016) 148–159.
[28] M.R. Dawson, D.G. Duda, S.S. Chae, D. Fukumura, R.K. Jain, VEGFR1 activity modulates myeloid cell infiltration in growing lung metastases but is not required for spontaneous metastasis formation, PLoS One 4 (2009) e6525.
[29] G.J. Russell-Jones, S.W. Westwood, A.D. Habberfield, Vitamin B12 mediated oral delivery systems for granulocyte-colony stimulating factor and erythropoietin, Bioconjug. Chem. 6 (1995) 459–465.
[30] P. Tuma, A.L. Hubbard, Transcytosis: crossing cellular barriers, Physiol. Rev. 83 (2003) 871–932.
[31] R. Fowler, D. Vllasaliu, F.H. Falcone, M. Garnett, B. Smith, H. Horsley, C. Alexander, S. Stolnik, Uptake and transport of B(12)-conjugated nanoparticles in airway epithelium, J. Control. Release 172 (2013) 374–381.
[32] R. Fowler, D. Vllasaliu, F.F. Trillo, M. Garnett, C. Alexander, H. Horsley, B. Smith, I. Whitcombe, M. Eaton, S. Stolnik, Nanoparticle transport in epithelial cells: pathway switching through bioconjugation, Small 9 (2013) 3282–3294.
[33] A.O. Saeed, J.P. Magnusson, E. Moradi, M. Soliman, W. Wang, S. Stolnik, K.J. Thurecht, S.M. Howdle, C. Alexander, Modular construction of multifunctional bioresponsive cell-targeted nanoparticles for gene delivery, Bioconjug. Chem. 22 (2011) 156–168.
[34] C.J. Dix, I.F. Hassan, H.Y. Obray, R. Shah, G. Wilson, The transport of vitamin B12 through polarized monolayers of Caco-2 cells, Gastroenterology 98 (1990) 1272–1279.
[35] K.S. Ramanujam, S. Seetharam, M. Ramasamy, B. Seetharam, Expression of cobalamin transport proteins and cobalamin transcytosis by colon adenocarcinoma cells, Am. J. Physiol. 260 (1991) G416–422.
[36] G.J. Russell-Jones, L. Arthur, H. Walker, Vitamin B12-mediated transport of nanoparticles across Caco-2 cells, Int. J. Pharm. 179 (1999) 247–255.
[37] K.B. Chalasani, G.J. Russell-Jones, A.K. Jain, P.V. Diwan, S.K. Jain, Effective oral delivery of insulin in animal models using vitamin B12-coated dextran nanoparticles, J. Control. Release 122 (2007) 141–150.
[38] R. Kozyraki, O. Cases, Vitamin B12 absorption: mammalian physiology and acquired and inherited disorders, Biochimie 95 (2013) 1002–1007.
[39] R. Green, L.H. Allen, A.-L. Bjørke-Monsen, A. Brito, J.-L. Guéant, J.W. Miller, A.M. Molloy, E. Nexo, S. Stabler, B.-H. Toh, P.M. Ueland, C. Yajnik, Vitamin B12 deficiency, Nat. Rev. Dis. Primers 3 (2017) 17040.
[40] C. Gherasim, M. Lofgren, R. Banerjee, Navigating the B12 road: assimilation, delivery, and disorders of cobalamin, J. Biol. Chem. 288 (2013) 13186–13193.
[41] C.R. Benoit, A.E. Stanton, A.C. Tartanian, A.R. Motzer, D.M. McGaughey, S.R. Bond, L.C. Brody, Functional and phylogenetic characterization of noncanonical vitamin B12–binding proteins in zebrafish suggests involvement in cobalamin transport, J. Biol. Chem. 293 (2018) 17606–17621.
[42] S. Bose, S. Seetharam, N.M. Dahms, B. Seetharam, Bipolar functional expression of transcobalamin II receptor in human intestinal epithelial Caco-2 cells, J. Biol. Chem. 272 (1997) 3538–3543.
[43] O. Aseem, J.L. Barth, S.C. Klatt, B.T. Smith, W.S. Argraves, Cubilin expression is monoallelic and epigenetically augmented via PPARs, BMC Genomics 14 (2013) 405.
[44] R. Respaud, L. Vecellio, P. Diot, N. Heuzé-Vourc'h, Nebulization as a delivery method for mAbs in respiratory diseases, Expert Opin. Drug Deliv. 12 (2015) 1027–1039.
[45] P.J. Borm, W. Kreyling, Toxicological hazards of inhaled nanoparticles–potential implications for drug delivery, J. Nanosci. Nanotechnol. 4 (2004) 521–531.
[46] K. Donaldson, V. Stone, C.L. Tran, W. Kreyling, P.J. Borm, Nanotoxicology, Occup. Environ. Med. 61 (2004) 727–728.
[47] P.H. Pandya, D.S. Wilkes, Complement system in lung disease, Am. J. Respir. Cell Mol. Biol. 51 (2014) 467–473.
[48] D. Filpula, H. Zhao, Releasable PEGylation of proteins with customized linkers, Adv. Drug Del. Rev. 60 (2008) 29–49.
[49] M. Takano, Y. Koyama, H. Nishikawa, T. Murakami, R. Yumoto, Segment-selective absorption of lysozyme in the intestine, Eur. J. Pharmacol. 502 (2004) 149–155.
[50] E.V. Seliverstova, N.P. Prutskova, Receptor-mediated endocytosis of lysozyme in renal proximal tubules of the frog Rana temporaria, Eur. J. Histochem. 59 (2015) 2482.
[51] F. Meng, G.H. Engbers, J. Feijen, Polyethylene glycol-grafted polystyrene particles, J. Biomed. Mater. Res. A. 70 (2004) 49–58.
[52] A. Alshehri, A. Grabowska, S. Stolnik, Pathways of cellular internalisation of liposomes delivered siRNA and effects on siRNA engagement with target mRNA and silencing in cancer cells, Sci. Rep. 8 (2018) 3748.
[53] H. Ayame, N. Morimoto, K. Akiyoshi, Self-assembled cationic nanogels for intracellular protein delivery, Bioconjugate Chem. 19 (2008) 882–890.
[54] S. De Koker, B.G. De Geest, C. Cuvelier, L. Ferdinande, W. Deckers, W.E. Hennink, S.C. De Smedt, N. Mertens, In vivo cellular uptake, degradation, and biocompatibility of polyelectrolyte microcapsules, Adv. Funct. Mater. 17 (2007) 3754–3763.
[55] A. Beyerle, A. Braun, A. Banerjee, N. Ercal, O. Eickelberg, T.H. Kissel, T. Stoeger, Inflammatory responses to pulmonary application of PEI-based siRNA nanocarriers in mice, Biomaterials 32 (2011) 8694–8701.
[56] H.P. Patil, D. Freches, L. Karmani, G.A. Duncan, B. Ucakar, J.S. Suk, J. Hanes, B. Gallez, R. Vanbever, Fate of PEGylated antibody fragments following delivery to the lungs: influence of delivery site, PEG size and lung inflammation, J. Control. Release 272 (2018) 62–71.
[57] M.C. Jones, S.A. Jones, Y. Riffo-Vasquez, D. Spina, E. Hoffman, A. Morgan, A. Patel, C. Page, B. Forbes, L.A. Dailey, Quantitative assessment of nanoparticle surface hydrophobicity and its influence on pulmonary biocompatibility, J. Control. Release 183 (2014) 94–104.
[58] A. Kumar, L.A. Dailey, B. Forbes, Lost in translation: what is stopping inhaled nanomedicines from realizing their potential? Ther. Deliv. 5 (2014) 757–761.
[59] A. Yamamoto, S. Okumura, Y. Fukuda, M. Fukui, K. Takahashi, S. Muranishi, Improvement of the pulmonary absorption of (Asu1,7)-eel calcitonin by various absorption enhancers and their pulmonary toxicity in rats, J. Pharm. Sci. 86 (1997) 1144–1147.
[60] R.U. Agu, M.I. Ugwoke, M. Armand, R. Kinget, N. Verbeke, The lung as a route for systemic delivery of therapeutic proteins and peptides, Respir. Res. 2 (2001) 198–209.
[61] L. Heinemann, W. Klappoth, K. Rave, B. Hompesch, R. Linkeschowa, T. Heise, Intra-individual variability of the metabolic effect of inhaled insulin together with an absorption enhancer, Diabetes Care 23 (2000) 1343–1347.
[62] M. Morello, C.L. Krone, S. Dickerson, E. Howerth, W.A. Germishuizen, Y.L. Wong, D. Edwards, B.R. Bloom, M.K. Hondalus, Dry-powder pulmonary insufflation in the mouse for application to vaccine or drug studies, Tuberculosis 89 (2009) 371–377.
[63] N. Wauthoz, P. Deleuze, J. Hecq, I. Roland, S. Saussez, I. Adanja, O. Debeir, C. Decaestecker, V. Mathieu, R. Kiss, K. Amighi, In vivo assessment of temozolomide local delivery for lung cancer inhalation therapy, Eur. J. Pharm. Sci. 39 (2010) 402–411.
[64] C. Gabay, Interleukin-6 and chronic inflammation, Arthritis Res. Ther. 8 (2006) S3.
[65] K. Ren, R. Torres, Role of interleukin-1beta during pain and inflammation, Brain Res. Rev. 60 (2009) 57–64.
[66] C. Alexander, E.T. Rietschel, Bacterial lipopolysaccharides and innate immunity, J. Endotoxin Res. 7 (2001) 167–202.
[67] I.M. El-Sherbiny, N.M. El-Baz, M.H. Yacoub, Inhaled nano- and microparticles for drug delivery, Glob. Cardiol. Sci. Pract. 2015 (2015) 2.
[68] C. Duret, N. Wauthoz, R. Merlos, J. Goole, C. Maris, I. Roland, T. Sebti, F. Vanderbist, K. Amighi, In vitro and in vivo evaluation of a dry powder endotracheal insufflator device for use in dose-dependent preclinical studies in mice, Eur. J. Pharm. Biopharm. 81 (2012) 627–634.
[69] V. Capel, D. Vllasaliu, P. Watts, P.A. Clarke, D. Luxton, A.M. Grabowska, G. Mantovani, S. Stolnik, Water-soluble substituted chitosan derivatives as technology platform for inhalation delivery of siRNA, Drug Deliv. 25 (2018) 644–653.
[70] D. Li, Y. Li, G. Li, Y. Zhang, J. Li, H. Chen, Fluorescent reconstitution on deposition of PM2.5 in lung and extrapulmonary organs, Proc. Natl. Acad. Sci. U. S. A. 116 (2019) 2488–2493.